DEAD BAND METHOD FOR SOLAR IRRADIANCE AND POWER RAMP DETECTION ALGORITHMS

David M. Willy
Ana Dyreson
Thomas L. Acker, Ph.D.
Eric Morgan, Ph.D.
Northern Arizona University
15600 South McConnell Drive
Flagstaff, AZ 86011
David.Willy@nau.edu
anadyreson@nau.edu
Tom.Acker@nau.edu
Eric.Morgan@nau.edu

Ronald K. Flood
Senior Consulting Engineer
Arizona Public Service Company
Technology Assessment and Interconnection
400 N. 5th Street, MS 9659
Phoenix, AZ 85004
Ronald.Flood@aps.com

ABSTRACT

Integration of solar photovoltaic (PV) power plants onto the electric utility grid can pose some challenges from the perspective of operating the power system (balancing load and demand) and in interconnecting a PV power plant (controlling distribution system voltage variations and thus power quality). An issue of particular importance is the rate at which the solar irradiance changes, and the consequent rate at which the power output changes, i.e. the ramp rates. Pertinent information describing the ramps is the frequency, duration, and magnitude of the ramps. This paper compares different methods of computing ramp rates in both irradiance and power. The "dead band" method, an historical data compression technique, is demonstrated for identifying fluctuations in the one second to several second timeframe. Ramp calculation methods are presented along with the results describing ramp events for two case studies.

1. INTRODUCTION

Grid integration of solar and wind energy consists of all that is required in order to connect, or integrate, these specific energy conversion systems into a high voltage transmission system - which is constantly balancing load and demand. In a system composed entirely of conventional generators, all of the generators are balanced to constantly meet the load. When any variable generation technology such as wind power or solar PV is added, changes in variable generation power output must be compensated for by adjusting the output of the conventional generation so that the net load – load minus variable generation – is met and system frequency kept constant. Similarly, interconnection is all that is required to connect solar or wind power plants to a distribution grid. At this lower-voltage (with respect to transmission voltages), and smaller scale level of the electric grid, the major concern is that changes in PV power output cause voltage fluctuations which must be compensated for. These variable resources impact grid operation on several different timescales. First, the longest timeframe defined here is unit commitment which can range from several hours to a few days ahead and consists of the required planning within that timeframe. Poor planning, by over- or under-estimating the load can result in higher operational costs. The second timeframe of interest is called Scheduling which is the day-ahead planning of all generation units to meet the forecasted load. Together, Unit Commitment and Scheduling consist of the bulk of the planning in order to meet the load. Next, Load Following is in the timeframe of a few minutes to a few hours and is in response to the specific diurnal (daily) load pattern. And finally, Regulation occurs in the seconds to several minutes timeframe and consists of the immediate response to the load by observing and maintaining system frequency.

One way of understanding variability on these timescales is by performing a ramp analysis. A ramp analysis concerns the "ramp rates" of the PV power fluctuations and the frequency and duration of these "ramp events." In determining the ramp rates and ramp events that must be dealt with on a transmission or distribution line, it is first

important to define them. A ramp rate is defined simply as the rate at which power fluctuates over time:

$$ramp\ rate = \frac{\Delta P}{\Delta T}$$

Here, ΔP is the change in power over time period ΔT. It now becomes important to define a ramp event; that is, come up with a method to define the starting and ending point of a ramp, and thus the magnitude of power change and duration of the ramp.

The basic reason for defining ramp events and determining ramp rates is to answer the following questions:

1) What are the characteristics of typical ramps that will occur at the PV power plant?
2) What is the worst case scenario ramp events observed at the PV power plant?

Note, in every case, the ramp events presented here should be combined with the ramps in the load to determine the fluctuation in "net load" that need to be handled at the system level.

2. RAMP DETECTION METHODS

No single ramp definition has been adopted in the wind or solar industry. Analyses often use "fixed-point" type methods that only detect ramps of fixed timescales. For example, in the analysis of wind power ramps, the change in power between subsequent ten minute averaged data points can be calculated which provide a series of ramps that are all ten minutes in duration but have different ramp magnitudes. However, advanced methods can detect ramp events of varying timescales by using a more complex ramp definition. Three of these methods were considered: the piecewise linearization "arc-chord" method, the "swinging door" method (sometimes called the "swinging window"), and the "dead-band" compression method.

2.1 Arc-chord

The "arc-chord" method (Horst & Beichl, 1996) measures the arc of the data and the direct chord length between points, and using a maximum threshold value declares a ramp event when the difference between the arc and the chord exceeds the threshold value.

2.2 Swinging door

The "swinging door" method (Makarov, Loutan, Ma, & de Mello, 2009, May) is more commonly used than the arc-chord method. It has recently been used in solar (Hansen, Stein, & Ellis, 2010) and wind (Florita, Hodge, & Orwig, 2013) to detect ramp events. It uses a vertical tolerance or error band to determine the "hinge" of the swinging door beginning at the first data point, and then "doors" are opened from the hinges to the second data point, see Fig. 1. The process is continued from one point to the next, each time saving the most "wide-open" setting that has been used for the door on either side. When the two doors become parallel or greater, the final point is considered the end of that ramp event and the beginning of a new ramp event.

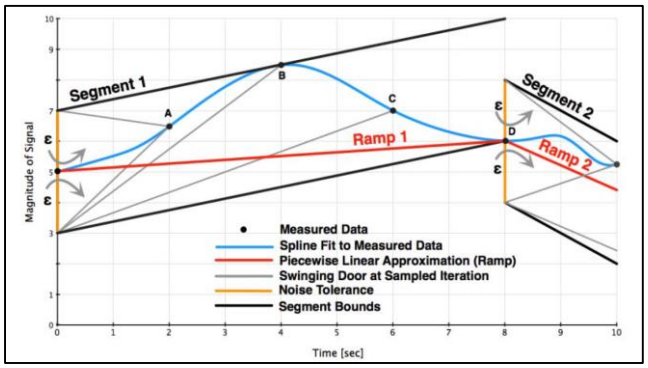

Fig. 1 "Swinging door" data compression method *(Florita, Hodge, & Orwig, 2013)*.

2.3 Dead band

Another data compression method is the "dead band" (EVSystems) method where error bands are used to create high and low angle tolerances for the following data point. The "swinging door" and "dead band" methods are similar to each other in their results. The "dead band" method is demonstrated in this study as an alternative to the swinging-door method having similar results and computational requirements.

The "dead band" method is applied as demonstrated in Fig. 2 and Fig. 3. To perform this method in a forward looking, time-preserving fashion, an aperture window is created for each error band used. These aperture windows, shown in Fig. 3, have a high and low angles as bounds created by drawing a line between the last turning point and the bounds of the error band of the last point. Next a line is drawn between the last turning point and the new point. If the angle of the new point is outside the bounds, then the previous point is the new turning point. If the angle is within the bounds, then the process continues to the next point. As the process continues, the angles bounding the critical aperture tighten based on the lowest high-angle and highest low-angle of the process, until a turning point is identified. Once a turning point is identified, the aperture

angles are reset, the points between the turning points are removed, and the process continues to the next data point.

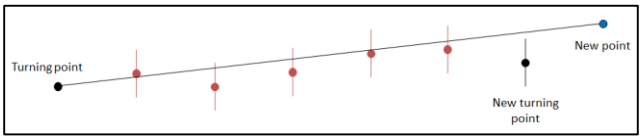

Fig. 2 The "dead band" data compression method, adapted from *(Freidenthal, 2014)*.

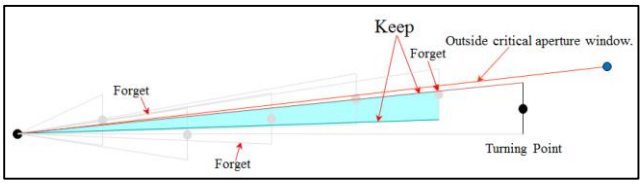

Fig. 3 Aperture windows created to identify turning points, adapted from *(Freidenthal, 2014)*.

3. RESULTS

Two case studies are considered; irradiance ramp results detected in a point-measured irradiance dataset and power ramp results detected in a power time series of a 2.66 MW power plant at a different location, which is also in Arizona.

3.1 Ramps in Irradiance Time Series

As an example of dead band ramp detection on irradiance time series, this section considers results from a wind and solar variability study completed by Northern Arizona University and NextEra Energy Resources,LLC. The goal of that study was to quantify the solar and wind variability at a location north of Flagstaff, AZ. The solar sensors were industry standard LI-COR type 200S irradiance sensors and measured total solar irradiance on a horizontal surface in W/m^2.

The sensitivity of the algorithm, and thus the number, magnitude, and duration of the ramps it identifies, is selected prior to implementing the ramp on the full data set. This value was selected through trial and error, by visually identifying that the ramps identified by the algorithm appeared to fit the data well. Fig. 5 and Fig. 6 (next page) show examples of how the width of the dead band changes the ramps which the algorithm identifies. After testing multiple dead band values on different days, a 25 W/m^2 dead band was selected.

The dead band ramp detection algorithm was used to identify ramp events in the 365 day irradiance time series.

The ramp algorithm identified ramps from 50 minutes after sunrise to 50 minutes before sunset. This time period was chosen for consistency with a model which was used later in the study for spatial smoothing analysis. Omission of the ramps that occur close to sunrise and sunset is not expected to exclude any significant events since ramps during these time periods are expected to be very small in magnitude. Fig. 4 shows the results of the ramp algorithm for one example day. The upper portion of Fig. 4 shows the raw irradiance data and the results of the dead band ramp detection. The middle portion of the figure shows the magnitude of the each ramp event throughout the day. For example, from 8 to 10 AM two long, large positive ("up") ramps dominate with several short negative ("down") ramps that begin shortly after 9 AM. The lower portion of the figure shows the ramp rates. The ramp rates indicate that the large positive ramps from 8-10 AM have a small ramp rate since they occur slowly, over the course of about an hour each. Since long, slow, ramps are simply reflections of the sun's predictable movement throughout the day, these long, slow ramps are not necessarily of interest. Ramps which have a large ramp rate represent short cloud movements and were of more interest for this variability study. Summaries of the ramp results always consider both the ramp duration and magnitude in order to differentiate between these short, fast ramps and long, slow ramps.

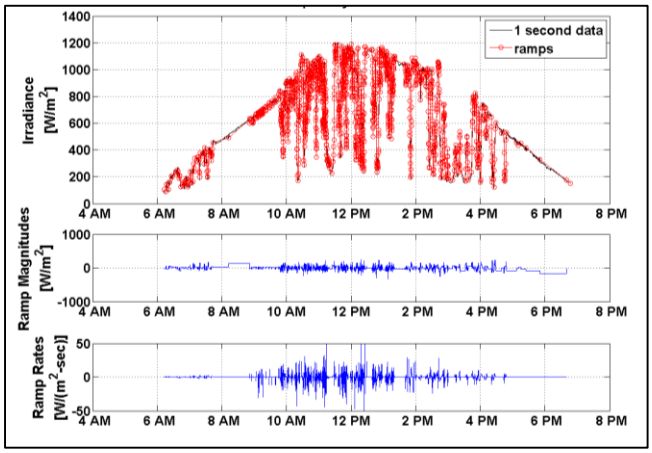

Fig. 4: The ramps detected on June 25th, 2012 are examined by considering the raw ramps (top), the magnitude of ramps (middle), and the ramp rates (bottom).

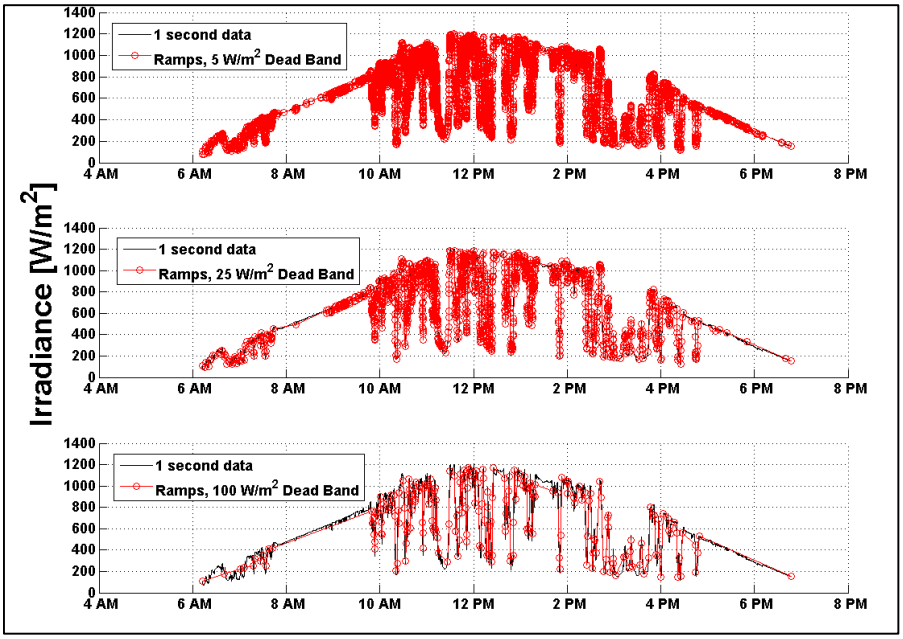

Fig. 5: Ramp detection is tested with 5, 25, and 100 W/m^2 dead bands. The 5 W/m^2 deadband captures many short ramps while the 100 W/m^2 deadband does not.

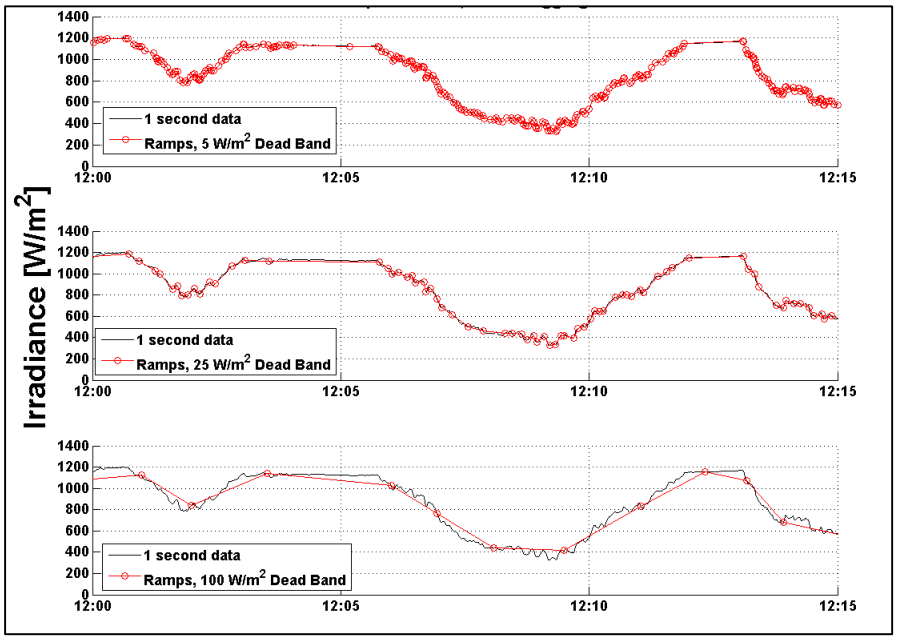

Fig. 6: Ramp detection with 5, 25, and 100 W/m^2 dead bands are examined over a 15 minute period in order to determine which algorithm is detecting the short ramps of interest.

The ramp algorithm was implemented on the 365 day irradiance time series. Fig. 7 shows the ramp duration, magnitude, and probability of occurrence. Here the probability is the number of ramps which fall into a given duration-magnitude bin divided by the total number of ramps detected in the dataset. Note that the ramp distributions for irradiance are only determined based on irradiance measurements at a single point sensor, not including smoothing effects which occur as irradiance is absorbed over the extent of a PV power plant. For this reason the ramp distribution in irradiance shown is expected to show more short-timescale variability than actual PV power output would.

While Fig. 7 provides information about the distribution of ramps, indicating which ramps are most likely to occur, Fig. 7 represents the magnitude of the most extreme ramp events by duration, for those less than two minutes long.

Note that as the durations increase from several minutes to hours (not shown), the magnitude of the ramps generally increases. These long duration changes, however, are simply a result of the sun's predictable motion through the sky. It is the shorter duration ramps (less than a few minutes) which are of more interest.

Here ramp events are considered "extreme" if their magnitude is above the 90th, 95th, 99th, or 99.5th percentile of the ramps in the same duration bin. For example, in Fig. 7, for ramps from zero to 10 seconds long, the most extreme ramps are those above the 99.5th percentile which have a magnitude of about 350 W/m^2 or those below the 5th percentile which have a value of -350 W/m^2. Generally, this symmetry is expected as clouds can induce both a fast decrease in irradiance as well as a fast increase in irradiance on their path over a sensor.

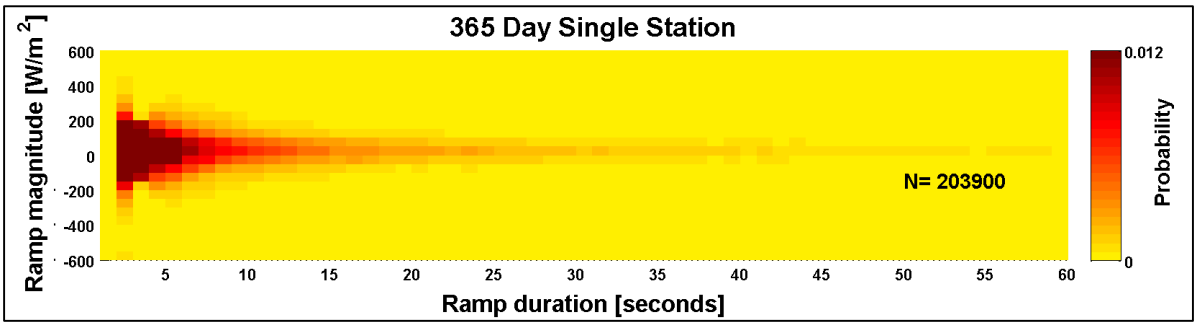

Fig. 7: A heat map is used to show the distribution of irradiance ramps by duration and magnitude. 'N' indicates the total number of ramps in the 365-day dataset. The heat map focuses on the short ramps of under one minute in duration, although the ramps detected (N) includes ramps of up to several hours in length on clear days.

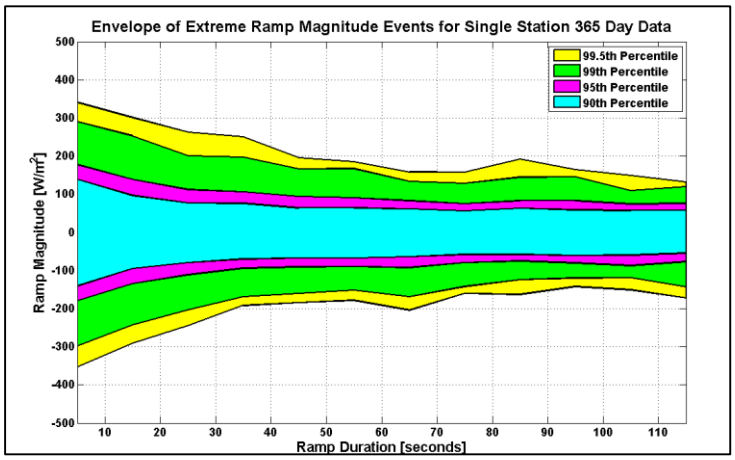

Fig. 7: The extreme irradiance ramp events are examined for the shortest duration ramps of less than two minutes. The extreme ramp magnitudes decrease ranging from 10 seconds to two minutes in durations, indicating that the largest ramps in this timescale occur at the shortest durations, and so will also have large ramp rates.

3.2 Ramps in the Power Time Series

While irradiance ramps provide interesting insight into solar resource variability, it is the power ramps which are of most concern to operators. This section shows how the same dead band ramp algorithm can be used on power time series using results from the Prescott airport solar facility solar variability study (Flood, Acker, Willy, Lemer, & Vandervoort, 2011). This project was completed by Northern Arizona University (NAU) with Arizona Public Service Company (APS) in order to explore the inherent output variability from 2.66 MW of solar PV installed at the APS's Prescott Airport PV Power Plant. 1-second power data from March, and April, and May 2011 were combined into one dataset to be analyzed.

The algorithm was performed using a dead band equal to ~5% of 2.66 MW nameplate capacity of the plant. As with the irradiance example, this value was selected through trial and error, by visually identifying that the ramps identified by the algorithm appeared to fit the data well. This value of 5% may be different for other PV power plants, depending on site specific variability and plant size, but is adequate for this analysis. Thus, the error band is equal to 125 kW (62.5 kW above and below the data point). As displayed in Fig. 8, which shows the underlying 1-second data and the ramps that were identified, the "dead-band" method appears to capture the actual ramps observed. Fig. 9 shows a histogram of the ramps that occurred on March 7, 2011 (a cloudy day).

The resulting histogram of ramps detected over the three month period is shown in Fig. 10 with numerical results in Table 1. As demonstrated in the histograms, the dead band algorithm (as implemented with the 5% error band) identifies primarily short duration (< 1 min) ramps, some of which are of large magnitude. The longer duration ramps identified are typically over periods when there is not a large change in output. For the values in Table 1, it is important to know that the values were generated for the magnitude and ramp rate by using the absolute value of the data (excluding the minimum values). This was done because of the relatively similar distribution of positive and negative ramp events (even though a few negative ramps far exceeded the positive ramps). As presented in Table 1, the average duration of the ramps identified over the three-month period of March, April and May was 147 seconds, the average of the absolute value of the magnitude was 171 kW, and the average of the absolute value of the ramp rate was 13 kW/sec. Furthermore, 99.7% of the of the absolute value of the ramp rates were less than 163 kW/sec, and the maximum ramp rates identified were -417 kW/sec (down ramp) and +231 kw/sec (up ramp). In Table 1, in the cells that indicate the maximum duration of the ramps, note that the maximum ramp duration is very long on the order of 27,000 seconds (~7.5 hours). This is due to the output of the power plant being limited to 2.66 MW by the power inverters (the DC capacity was designed to be higher than the AC capacity), and that in turn causing the power output to be clipped across the middle of the day on relatively sunny days. (The panels are rated at ~3.0 MW while the inverter total is rated at ~2.5 MW.) This in turn creates one very long shallow ramp across the middle of some days.

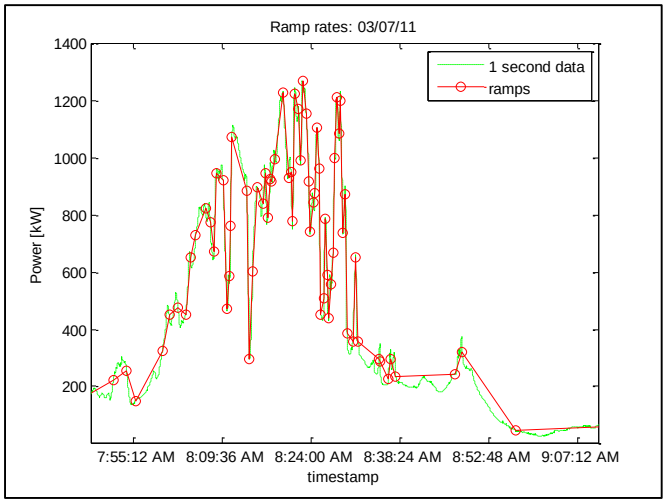

Fig. 8: Example of power ramps identified using the "dead band" method. Each ramp begins and ends with an open circle, and is connected by the solid red line.

TABLE 1: A summary of important numerical results pertaining to ramps tabulated for the months of March, April, and May 2011.

		units	σ	Avg	Min	Max	95.50%	99.00%	99.70%	99.90%
March, April, and May	duration	seconds	739	147	1	28263	558	2489	5431	10170
	magnitude	kW	239	171	-1941	2064	500	779	1082	1380
	ramp rate	kW/sec	27.0	13.0	-417	231	57.7	132	163	186

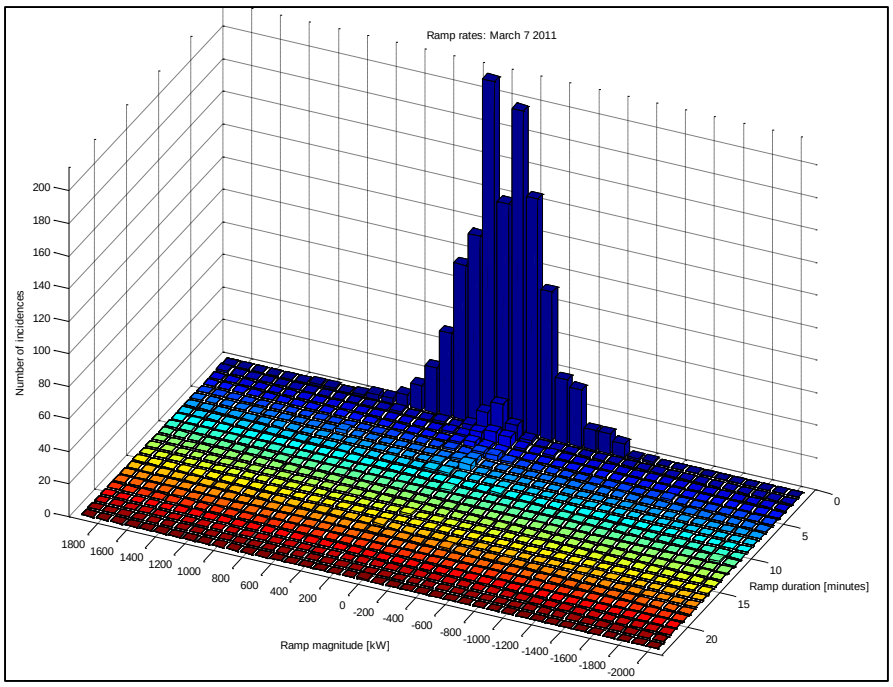

Fig. 9: A histogram of ramp events using the dead band method for March 7, 2011 (a cloudy day).The ramps are concentrated at around 1-minute durations with ramp magnitudes frequently existing between -600 and +600 kW.

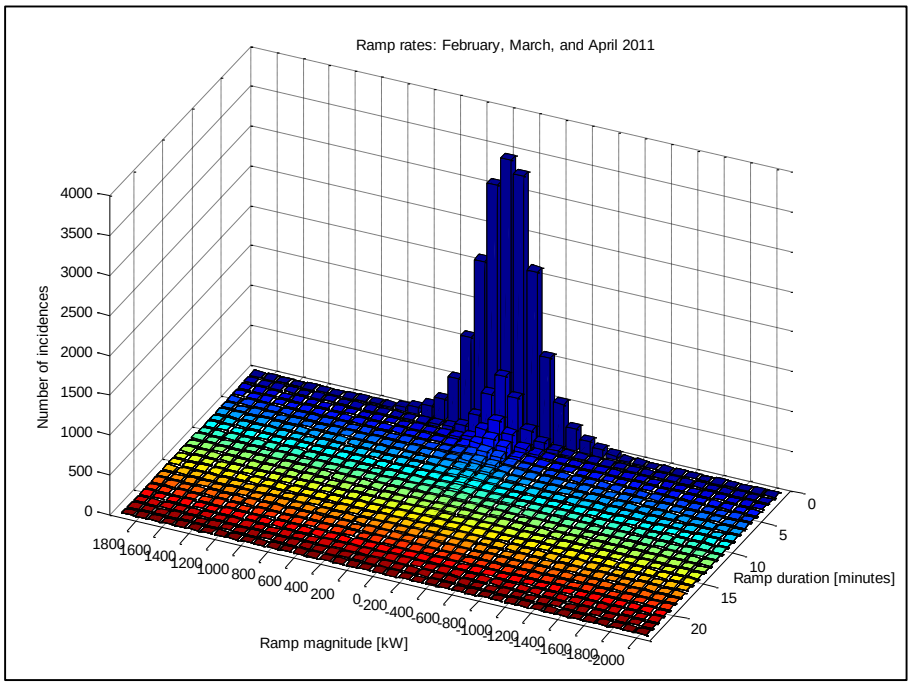

Fig. 10: A histogram of ramp events for the months of March, April and May 2011. The ramp durations are concentrated around one minute with ramp magnitudes between -600 and +600 kW occurring most frequently.

5. CONCLUSION

A dead band technique was proposed to identify irradiance and power ramp rates. Two case studies were included; one for detecting irradiance ramps and one for detecting power ramps from a solar PV plant. This technique was found to sufficient in resolving rapid variations in power that can occur at a PV power plant. Ramp rates and ramp durations can be tabulated in histograms, tables, heat maps, envelope plots, and contour plots to characterize the ramping behavior of the solar resource or of a power plant. The dead band method is expected to be computationally similar to the swinging door method, and both are able to capture ramps at a variety of timescales. The dead band method (not unlike the swinging door method) requires pre-calibrating the algorithm to determine the sensitivity to ramp detection. This calibration requires judgment by the user in determining what type of ramp events are of interest for a particular application, making it tunable to the user's needs.

6. REFERENCES

EVSystems. (n.d.). *Historian Data Compression.* Retrieved July 2011, from EVSystems: www.evsystems.net/files/Historian_Data_Compression.doc

Flood, R. K., Acker, T. L., Willy, D. M., Lemer, J., & Vandervoort, A. (2011). *Prescott airport solar facility solar variability study.* Retrieved from http://www.aps.com/library/renewables/PrescottVariability.pdf

Florita, A., Hodge, B.-M., & Orwig, K. (2013). Identifying Wind and Solar Ramping Events. *IEEE Green Technologies Conference* (pp. 147-152). Corpus Christi, Texas: IEEE.

Freidenthal, S. (2014, 5 29). Retrieved from EVSystems: www.evsystems.net/files/GE_Historian_Compression_Overview.ppt

Hansen, C. W., Stein, J. S., & Ellis, A. (2010). *Statistical Criteria for Characterizing Irradiance Time Series.* Albuquerque, New Mexico: Sandia National Laboratories, SAND2010-7314.

Horst, J. A., & Beichl, I. (1996). Efficient piecewise linear approximation of space curves using chord and arc length. *SME Applied Machine Vision '96 Conference.* Cincinnati, OH.

Makarov, Y. V., Loutan, C., Ma, J., & de Mello, P. (2009, May). Operational Impacts of Wind Generation on California Power Systems. *IEEE Transactions on Power Systems*, Vol. 24, No. 2, 1039-1050.